ACS Catalysis

Freie Universität Berlin

Subscriber access provided by UB + Fachbibliothek Chemie | (FU-Bibliothekssystem)

Article

Spectroscopic studies of how moisture enhances CO oxidation over Au/BN at ambient temperature

Tuyet-Mai Tran-Thuy, Chin-Chih Chen, and Shawn D Lin

ACS Catal., **Just Accepted Manuscript** • Publication Date (Web): 11 May 2017

Downloaded from http://pubs.acs.org on May 12, 2017

Just Accepted

"Just Accepted" manuscripts have been peer-reviewed and accepted for publication. They are posted online prior to technical editing, formatting for publication and author proofing. The American Chemical Society provides "Just Accepted" as a free service to the research community to expedite the dissemination of scientific material as soon as possible after acceptance. "Just Accepted" manuscripts appear in full in PDF format accompanied by an HTML abstract. "Just Accepted" manuscripts have been fully peer reviewed, but should not be considered the official version of record. They are accessible to all readers and citable by the Digital Object Identifier (DOI®). "Just Accepted" is an optional service offered to authors. Therefore, the "Just Accepted" Web site may not include all articles that will be published in the journal. After a manuscript is technically edited and formatted, it will be removed from the "Just Accepted" Web site and published as an ASAP article. Note that technical editing may introduce minor changes to the manuscript text and/or graphics which could affect content, and all legal disclaimers and ethical guidelines that apply to the journal pertain. ACS cannot be held responsible for errors or consequences arising from the use of information contained in these "Just Accepted" manuscripts.

ACS Publications

ACS Catalysis is published by the American Chemical Society. 1155 Sixteenth Street N.W., Washington, DC 20036

Published by American Chemical Society. Copyright © American Chemical Society. However, no copyright claim is made to original U.S. Government works, or works produced by employees of any Commonwealth realm Crown government in the course of their duties.

Spectroscopic studies of how moisture enhances CO oxidation over Au/BN at ambient temperature

*Tuyet-Mai Tran-Thuy, Chin-Chih Chen, Shawn D. Lin**

Department of Chemical Engineering, National Taiwan University of Science and Technology, Taipei 106, Taiwan

Abstract

Gold catalysts readily catalyze CO oxidation at sub-ambient temperature, wherein moisture can influence the activity typically with a volcano-shape dependency. In this study, we examine moisture-enhanced CO oxidation over Au/BN. The room-temperature CO oxidation activity of Au/BN increases quickly with increasing moisture content up to 100% relative humidity (RH). In situ DRIFTS (diffuse reflectance infrared fourier-transformed spectroscopy) and in situ UV-Vis-DRS (UV-visible diffuse reflectance spectroscopy) demonstrate mainly metallic gold presents on h-BN support. Surface intermediates are found when moisture is fed together with CO and O_2, attributable to $^*CO(H_2O)_n$ and $^*OOH$, respectively. These surface intermediates are reactive when purging counter reactant. Injection of isotope labeled $H_2{}^{18}O$ demonstrates that OH from H_2O takes part in the process of CO_2 formation. The results of this study provide direct evidences showing moisture-enhanced CO adsorption, moisture-enhanced O_2 adsorption, and their activation that can possibly lead to promotion of CO oxidation over Au/BN catalyst.

Keywords: Au/BN, moisture, CO oxidation, hydroperoxyl, intermediate.

1. Introduction

Many studies have reported that gold nanoparticles supported on metal oxides like TiO_2, Al_2O_3, Fe_3O_4 and CeO_2, etc. can catalyze CO oxidation at ambient and sub-ambient temperatures under nominal dry conditions.[1-4] However, moisture significantly influences catalyst activity[5-8] which can limit the applications of such high-activity Au catalysts. The CO oxidation activity over Au catalysts typically exhibits a volcano-shape dependency on moisture concentration. Moisture plays as a promoter at low concentration but as an inhibitor at high concentration. In the absence of O_2, no CO_2 could be detected under CO-H_2O co-feeding over Au/TiO_2[5] and Au/Al_2O_3[8] at the same room-temperature conditions of CO oxidation. This indicates that H_2O can influence CO oxidation over Au catalysts but is not a reactant for the formation of CO_2.

Bond and Thompson[9] proposed that CO adsorbed on metallic gold could interact with OH on Au^{3+} to form COOH surface species which would react with adsorbed O_2. Costello et al.[10] proposed that Au^+COOH (formate) from insertion of CO_{ad} into Au^+OH^- could react with hypothesized $^*O$ from O_2 adsorption to generate CO_2; the possible role of moisture may include activation of less active carbonate species.[11] Henao et al. reported an IR band at 1242 cm^{-1} during CO adsorption over Au/TiO_2 and assigned it to hydroxycarbonyl (COOH).[12] However, the band at around 1230 cm^{-1} that was found during CO_2 adsorption over Au/TiO_2[13] and during CO oxidation over Au/ZnO[14] was assigned differently. Smit et al.[15] proposed that water adsorption on metal oxide (Fe_2O_3) can generate OH which can interact with CO leading to formate ($HCOO_{ad}$) intermediate based on DRIFTS study. DFT calculation also suggested that the formation of hydroxycarbonyl species via direct interaction between $^*CO$ and $^*OH$ is facile over Co_3O_4 (100) and Pt (111).[16] Chen et al.[17] assigned the C-O vibration at 2158 cm^{-1} over Au/SiO_2 and Au/Ti-SiO_2 to $^*COOH$ species from CO interaction with OH. Li et al.[18] reported that formate (Au–COOH) and carbonate-like (Au–CO_3H) species observed in DRIFTS correlated with CO oxidation activity. All these results suggest the presence of COOH intermediate from H_2O-CO interaction but spectroscopic results are controversial.

Finch et al.[19] first proposed a $AuOOH \cdot xH_2O$ species based on Mossbauer spectroscopy and its synergistic interaction with ferrihydrite support resulting in high CO oxidation activity of Au-Fe catalyst at room temperature. Theoretical studies[20-23] of CO oxidation over gold catalysts suggested that O_2 activation is a key step and can occur via proton transfer from H_2O to form $^*OOH$ (hydroperoxyl), which then readily reacts with CO leading to CO_2 formation. The proton transfer from H_2O to O_2 on $Au_8/MgO(100)$[20] or on Au_{10} and Au_{38} cluster[21,23] can weaken O-O bond through the formation of superoxo state. Hydroperoxyl ($^*OOH$) intermediate over TiO_2 has been reported to show vibrational bands at 1220-1090 cm^{-1} for δ_{OO-H} and at 838 cm^{-1} for ν_{O-O}.[24-27] However, only few experimental observations of $^*OOH$ have been reported on Au/Fe_2O_3[19] and Au/TS1[28] by Mossbauer and UV-Vis spectroscopy, respectively.

The lack of spectroscopic evidence to the above-mentioned active intermediates on supported Au catalysts may be related to the hydrophilicity of oxide support which can lead to abundant adsorbed H_2O and OH density. The volcano-shape dependency on moisture indicates that promoting effect is counter balanced by increasing H_2O content (high RH).[5,7,8,22] Change in hydrophilicity of support surface can be a viable method to suppress the adverse effect of moisture on CO oxidation over Au catalysts and may consequently provide an opportunity to observe possible intermediates related to moisture enhancement. Herein, we use hexagonal boron nitride (h-BN), a hydrophobic support, for loading Au nanoparticles and examine the influence of moisture on CO oxidation at RT (room temperature). It is interesting to find that the CO oxidation activity of Au/BN can be enhanced by increasing moisture all the way to 100% RH at RT. The possible role of moisture on CO oxidation is examined by using in situ DRIFTS and in situ UV-Vis-DRS. The formation of surface species from the interaction of H_2O and CO and O_2 are reported. The results provide direct evidences that the promoting roles of H_2O include activating both CO and O_2 leading to enhancement in CO oxidation over Au/BN catalyst.

2. Experimental

2. 1. Catalyst preparation

Gold was loaded on h-BN (Alfa Aesar, 99.5%, 8 m^2/g) of 1 wt% Au by a deposition method. BN was suspended in H_2O-MeOH (1:1) and 2 M NH_3(aq) was added to maintain pH at around 10.5 when adding

$AuCl_3$(aq) (Aldrich, 99.99%). After aging at RT for 1 h, solid sample was filtered, washed with deionized water, dried under vacuum at room temperature, and calcined in air at 300^{o}C for 1 hour.

2. 2. Characterization

An inductively coupled plasma-atomic emission spectrometer (ICP-AES, Horiba Jobin Yvon, JY 2000-2) was used to analyze gold loading on BN based on liquid filtrate from Au/BN preparation. From ICP-AES results, the Au loading is confirmed as the expected 1.00 ± 0.03 wt%. TEM images were recorded using a Philips FEI Tecnai F30 HRTEM with an acceleration voltage of 200 kV. The mean particle size of Au was calculated by averaging over 200 particles in the recorded images. A commercial instrument (BELSORP-max) was used for measuring N_2 adsorption at -196 ^{o}C and moisture adsorption 30 ^{o}C, respectively. Samples were degassed under high vacuum at 200 ^{o}C for 12 h. A dual-isotherm test was carried out for moisture adsorption where in sample was be evacuated in high vacuum at 0.01 kPa at RT for 4h in between the 1st and the 2nd moisture adsorption measurements.

2. 3. CO oxidation tests

The CO oxidation reaction was conducted using 1% CO + 20% O_2 (balanced with He) with different partial pressures of moisture in a flow-type packed-bed microreactor system operated at atmospheric pressure and a space velocity of 163.7 μmol CO.g^{-1}catalyst.min^{-1}. All the gases passed through drying column before entering the reactor system. Water was introduced to the feed by using a syringe pump. Typically, 0.1 g as-prepared Au/BN sample was packed in reactor, pretreated in air from RT to 300 ^{o}C at 5 ^{o}C/min with 1 h dwelt time, then cooled to RT in N_2 flow. The reactor effluent was analyzed using an in-line GC with PDHID detector and packed columns of Porapak N and Molecular Sieve 5 A. The effluent typically showed a carbon balance of 100±5 %. While the CO conversion is typically below 25%, the reaction rate was calculated using a differential reactor model equation.

2. 4. In-situ DRIFTS

In-situ DRIFTS measurements were taken using an in-situ cell (Spectratech or Harrick Praying Mantis, with CaF_2 or ZnSe windows) and Nicolet 6700 FTIR spectrometer with a mercury-cadmium-telluride (MCT/A) detector. The catalyst calcined at 300^{o}C was loaded in IR cell and was pretreated again at 120^{o}C in air for 1 hour, then cool down to RT in N_2. Thereafter, a background spectrum was taken using

an accumulation of 64 scans and 4 cm^{-1} resolution. The reactant flow was introduced at the same conditions as CO oxidation reaction test at 100% RH, RT. CO gas phase signal was recorded at 1% CO in N_2 over low surface area quartz powders and was subtracted from the recorded spectrum over BN and Au/BN. $H_2{}^{18}O$ (Aldrich -Sigma) was used and compared with $H_2{}^{16}O$ by pulse injection into steady flows of CO, O_2, and CO+O_2 flow using in-situ DRIFTS analyses. $H_2{}^{16}O$ and $H_2{}^{18}O$ liquids were frozen and degased under N_2 flow for 30 minutes before uses.

2. 5. In situ UV-Vis-DRS

In-situ UV-Vis-DRS was carried out using in situ cell (Harrick, Praying Mantis) and Thermo Evolution 300 instrument with Xenon lamp at a 120 nm/min scan rate in the wavelength range of 200 to 900 nm. $BaSO_4$ was used to obtained spectrum baseline before all measurements. As-prepared Au/BN was loaded and calcined inline to 300 ^oC before cooling down to RT in N_2 and then a reference spectrum was recorded for further in-situ examination.

Results

3. 1. Effect of H_2O on CO oxidation over Au/BN

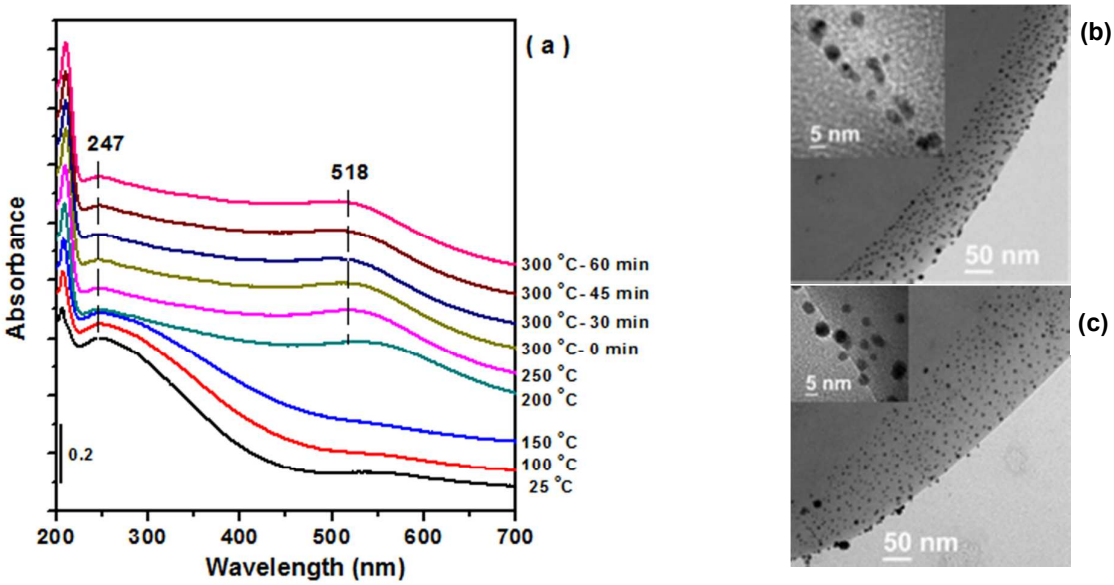

Figure 1. (a) In situ UV-Vis-DRS spectra during pretreatment of as-prepared Au/BN in air from RT to 300^oC, at a ramp rate of 5^oC/min, with $BaSO_4$ as the reference; TEM images of Au/BN (b) before and (c) after CO oxidation at RT.

The as-prepared Au/BN contained relatively strong LMCT (ligand metal charge transfer) band at 247 nm in UV-visible spectrum (Figure 1a), indicating mainly unreduced Au species. During calcination to 300 ^{o}C, the LMCT band decreased and SPR (surface plasmon resonance) band at 518 nm evolved (Figure 1a), indicating the conversion to metallic gold. The nearly constant band at around 210 nm can be assigned to h-BN support.[29,30] TEM images (Figure 1b) of the calcined Au/BN catalyst show that nano-size gold particles were located mainly at the edge of h-BN, and the number-averaged particle size was around 4 nm (Figure S1a, Supporting Information). No obvious change in Au particle size was found after CO oxidation test (Figure 1c). Water vapor adsorption over h-BN and over Au/BN was analyzed at 30 ^{o}C and the results show that Au/BN had a higher uptake than h-BN while both had only reversible uptakes (Figure S2, Supporting Information). Comparing to TiO_2 (rutile) of similar BET surface area (based on N_2 isotherm), both h-BN support and Au/BN catalyst had significantly lower monolayer uptake (Table S1, Supporting Information). This demonstrates that the BN support used in this study is more hydrophobic than oxides.

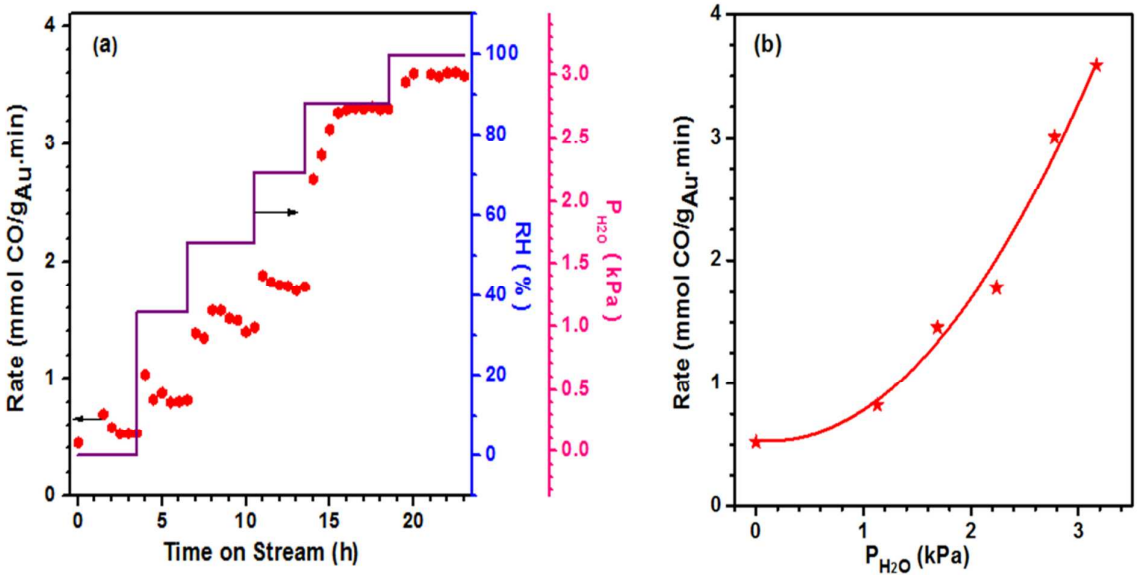

Figure 2. (a) Change in CO oxidation rate over Au/BN with increasing RH at RT; (b) the dependency of steady state CO oxidation rate on moisture partial pressure.

Room-temperature CO oxidation was examined over Au/BN with stepwise increase in RH (relative humidity) and the results are shown in Figure 2a. The rate increased with increasing moisture content up

to 100% RH. The dependency of steady state CO oxidation rate on water partial pressure shows a quick-rising trend (Figure 2b). No H_2 was detected in the reactor effluent wherein CO_2 was the sole product and CO_2 formation was not found when feeding only CO with moisture. This reveals that CO oxidation, not water gas shift reaction, led to the formation of CO_2. The results confirm the increasing moisture promotion of CO oxidation over Au/BN without saturated state up to 100% RH. In contrast, CO oxidation over oxide-supported Au catalysts typically shows a volcano curve dependency on moisture concentration and the decreased activity under high moisture content can be recovered by purge to decrease moisture content.[5,8,22] This indicates a probable reason of decreased activity over Au/oxide under high moisture content is formation of water overlayer on active sites of Au/oxide catalysts. The absence of inhibitory effect at high RH suggests that H_2O adsorption over Au/BN did not cause water layer over active sites. Moisture obviously plays a co-catalyst role during CO oxidation over Au/BN and its possible roles in enhancing the reaction were examined using spectroscopic methods as that will be shown below.

3. 2. In situ DRIFTS

Moisture can promote CO adsorption on Au/BN as indicated by the DRIFTS results shown in Figure 3a. Under nominal dry conditions, CO adsorption on Au/BN resulted in a sole absorbance peak at 2113 cm^{-1} in agreement with the reported CO adsorption on metallic Au.[13,15,31-33] There is no trace of CO adsorption on negatively or positively charged gold expected at around 2050-2081 cm^{-1} and 2120-2127 cm^{-1}, respectively,[34-36] indicating the absence of cationic or anionic Au species in Au/BN. When co-feeding moisture at 100% RH, an additional band at 2170 cm^{-1} appeared while the band at 2113 cm^{-1} did not change. The new band at 2170 cm^{-1} is attributed to adsorbed CO interacting with nearby H_2O and/or hydroxyl groups ($^*OH$) as discussed below.

Many earlier reports attributed an absorbance band at 2170 - 2179 cm^{-1} to CO adsorbed on metal oxide supports[17,37-40] or on cationic gold.[41,42] Neither assignment is applicable to Au/BN because that no such band was found over h-BN support or over Au/BN under nominal dry conditions. Water adsorption is weak on Au surface and no OH species would form even on step and edge sites[43-45] and therefore, transformation from Au^0 to $Au^{\delta+}$ just by the presence of moisture is unlikely to occur. Chen et al.[17] assigned a C-O vibration at 2158 cm^{-1} over Au/SiO_2 and Au/TiO_2 to $^*COOH$ (hydroxycarbonyl) species,

from CO interaction with OH. Figure 3b shows that the ν_{OH} band at 3750 cm^{-1} gradually shifted to 3696 cm^{-1} when purging CO over moisture-saturated Au/BN. This ν_{OH} at 3750 cm^{-1} can be ascribed to that of B-OH on h-BN surface[46,47] and consequently its shifting to lower wavenumber upon CO exposure demonstrates possible interaction between OH and CO_{ad} leading to formation of *COOH species. The presence of *COOH is often assigned with accompanied $\nu_{as,\,OCO}$ and $\nu_{s,\,OCO}$ centered at 1628 and 1377 cm^{-1}, respectively,[18,48,49] and δ_{OH} band at 1419 cm^{-1}.[18] In our DRIFTS analysis, $\nu_{as,OCO}$ and $\nu_{s,OCO}$ at around 1628 and 1377 cm^{-1}, respectively, could be barely identified by the peak envelope when CO was fed to moisture-saturated Au/BN, but the results are not convincing because of the noisy absorbance from moisture (Figure S4, Supporting Information). However, theoretical calculations indicated that the interaction between OH and CO over Au surface would cause a red shift in ν_{CO} band[50] and this argues against the assignment of *COOH for the observed 2170 cm^{-1} band. Another possible attribution of the ν_{OH} at 3750 cm^{-1} is the O-H stretching of water cluster and its shifting can be interpreted to change in water cluster size.[51,52] Thus, the observed shift in ν_{OH} can be explained by the formation of $^{*}CO(H_2O)_n$. DFT calculation indicated that the ν_{CO} band of $^{*}CO(H_2O)_n$ should be blue shifted[50], in consistent with the observed 2170 cm^{-1} band. The results indicate clearly the presence of interaction between CO_{ad} and surface H_2O.

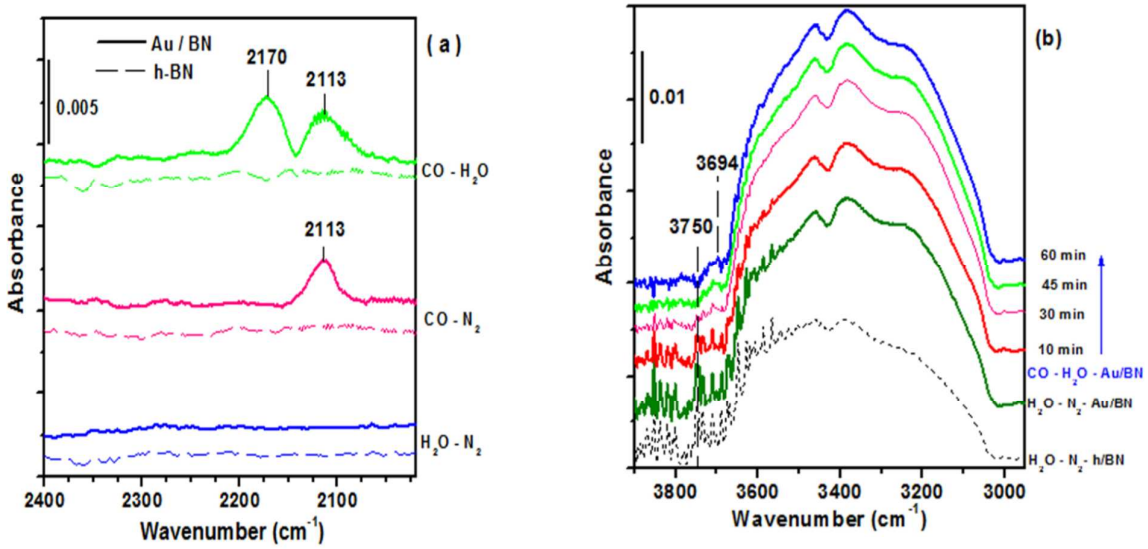

Figure 3. In situ DRIFTS while introducing CO over Au/BN (solid lines) and h-BN (dotted lines) under nominal dry and wet (100% RH) conditions.

Oxygen does not present observable IR absorbance band but protonated O_2 may have. The DRIFTS spectra in Figure 4 show obvious bands at 833, 943 and at 1220-1095 cm^{-1} with O_2–H_2O co-feeding. The protonation of O_2 by H_2O can lead to OOH (hydroperoxyl) species,[20-23] which is considered as the key step for O_2 activation over Au catalysts. Hydroperoxyl (*OOH) species can show vibrational bands at 1220-1090 cm^{-1} for $\delta_{OO\text{-}H}$ and at 838 cm^{-1} for $\nu_{O\text{-}O}$.[24-27] Nakamura et al.[27] attributed two new bands at 838 and 1250-1120 cm^{-1} to TiOOH, when peroxo $Ti(O)_2^*$ (represented by $\nu_{O\text{-}O}$ at 943 cm^{-1}) is transformed to hydroperoxyl (Ti^*OOH) by protonation. The $\nu_{O\text{-}O}$ of metal peroxo, $M(O_2)$, typically presents at 943-979 cm^{-1},[53,54] and the $\nu_{O\text{-}O}$ of superoxo metal complexes (M-O-OH) is typically at around 830-850 cm^{-1}.[27,55,56] Therefore, the observed vibration band at 943 cm^{-1} is assigned to $\nu_{Au(O2)}$ of surface peroxo on Au/BN. The band at 833 cm^{-1} is ascribed to $\nu_{O\text{-}O}$ while the band at 1250-1120 cm^{-1} can be contributed from the $\delta_{OO\text{-}H}$ of AuOOH.[27,55-57] This indicates the formation of *OOH through the protonation of O_2 by moisture on Au/BN. The observed bands of $\nu_{O\text{-}O}$ and δ_{OOH} lie at lower frequencies than those of free H_2O_2 (1270-1290 cm^{-1} for OOH bending and 865-850 cm^{-1} for O-O stretching vibration bands).[56-58]

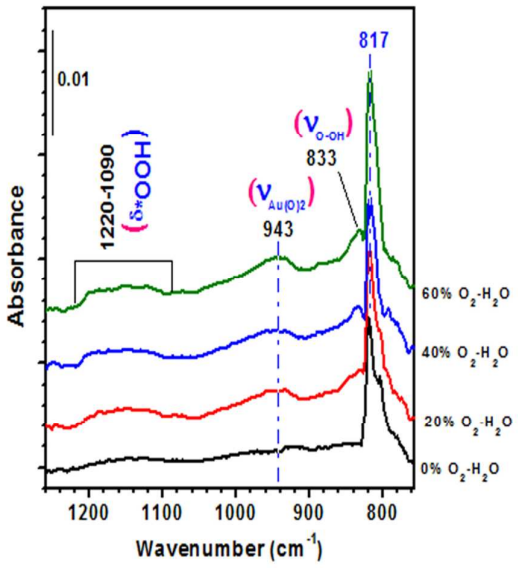

Figure 4. In situ DRIFTS spectra of Au/BN under moisture-O_2 flow; the vibrational bands suggesting the formation of *OOH species are indicated.

Figure 5 shows changes in in situ DRIFTS spectra when adding H_2O to nominal dry CO oxidation conditions over Au/BN at RT. Moisture resulted in observation of the above-mentioned bands at 2170 cm^{-1} and at 833 cm^{-1} with obvious increase in the intensity of CO_2 bands at 2362, 2336 cm^{-1}. The ν_{OH} at 3750 cm^{-1} was also observed when moisture was fed to nominal dry $CO-O_2$ flow following by a subsequent shift to 3695 cm^{-1} (Figure S5, Supporting Information), similar with that described in Figure 3b. The moisture-promoted $^*CO(H_2O)_n$ and $^*OOH$ formation may be attributed as the reason of enhanced CO_2 formation. To the best of our knowledge, this may be the first direct observation of moisture-promoted surface species of CO_{ad} and $^*OOH$ under CO oxidation conditions over Au catalysts.

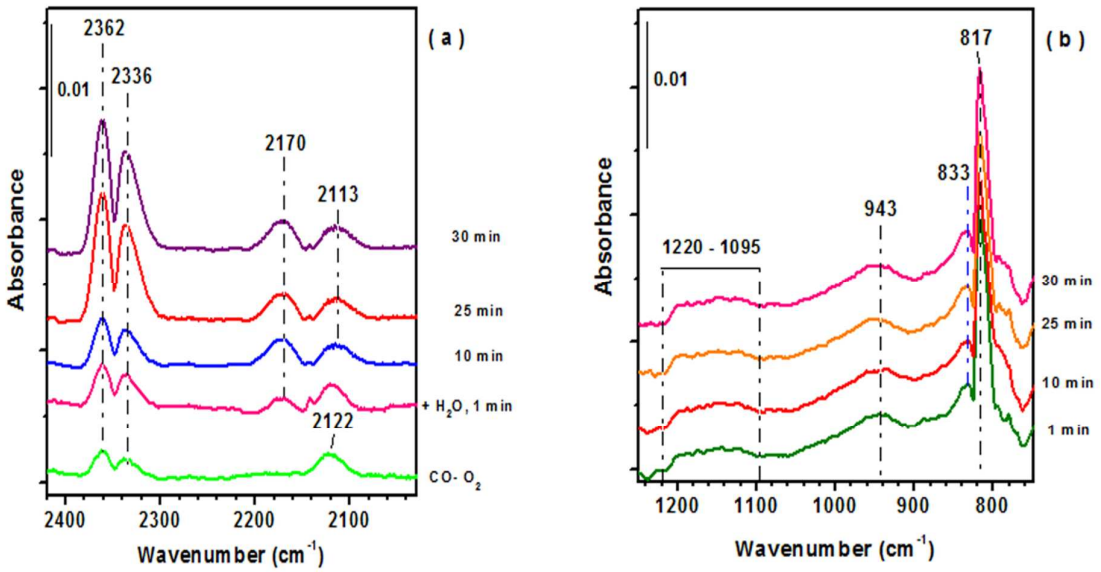

Figure 5. In situ DRIFTS spectra of Au/BN when introducing moisture (100% RH) to nominal dry CO oxidation reaction feed.

Figure 6 shows comparison of pulse water ($H_2{}^{16}O$ and $H_2{}^{18}O$) injection into CO, O_2, and $CO+O_2$ flow over Au/BN at RT. There was no obvious shift in the two bands at 2113 and 2170 cm^{-1} assigned to adsorbed CO and $^*CO(H_2O)_n$ species. Neither in the range of δ_{OO-H} at 1220 – 1190 cm^{-1} and ν_{O-OH} at 850 – 832 cm^{-1} could peak shift be observed (Figure 6b); this can be expected as that H_2O activated the adsorbed O_2 via proton transfer as described earlier. However, both $C^{16}O_2$ vibration at 2160 and 2336 cm^{-1} and $C^{18}O^{16}O$ vibration[59] at 2140 and 2123 cm^{-1} were found under pulse $H_2{}^{18}O$ injection into $CO+O_2$

flow over Au/BN (Figure 6a). This suggests that OH from H_2O takes part in the process of CO_2 ($C^{18}O^{16}O$) formation. Considering the possible reactions of the two intermediates $^*OOH$ and $^*CO(H_2O)_n$ (eqn 1and 2), this implies that eqn 2 may be a key step leading to CO_2 formation.

$$^*{}^{16}O^{16}OH + {}^*CO \xrightarrow{k_1} C^{16}O_2 + {}^*{}^{16}OH + (*) \qquad (1)$$

$$^*CO(H_2{}^{18}O)_n + {}^*{}^{16}O_2 \xrightarrow{k_2} {}^*CO^{18}OH + {}^*{}^{16}O^{16}OH + (n-1)H_2{}^{18}O \qquad (2)$$

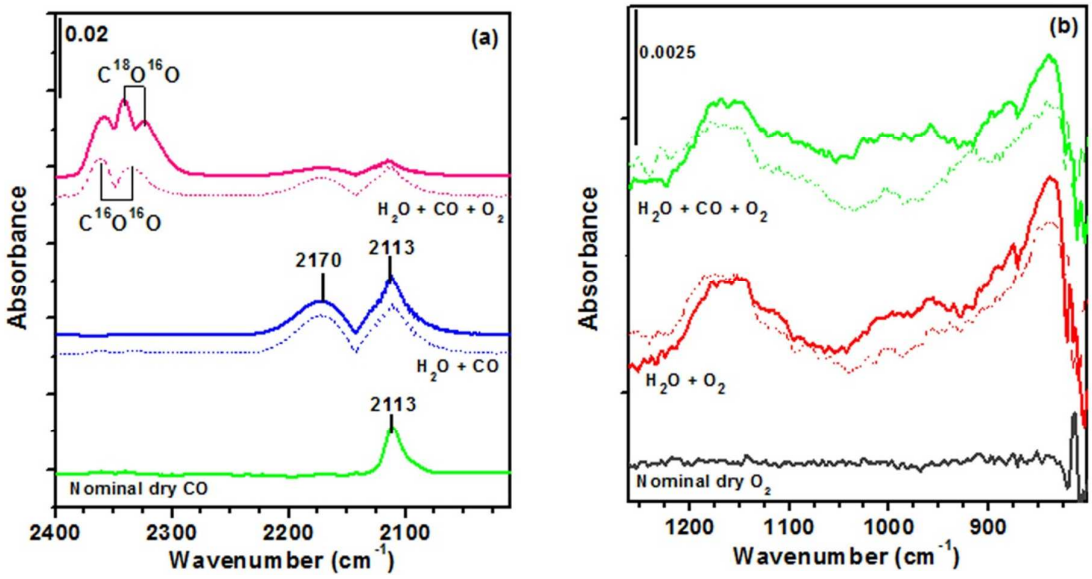

Figure 6. In situ DRIFTS of pulse injection of $H_2{}^{18}O$ (solid line) into CO, O_2, and CO+O_2 flow over Au/BN at RT. The spectra from $H_2{}^{16}O$ pulse injections are shown in dotted lines for comparison.

3. 3. In situ UV-Vis-DRS

In situ UV-Vis-DRS analysis was carried out using Au/BN under dry N_2 as the reference, in order to learn how moisture and gas adsorption may influence electron density of Au. Figure 7a shows that CO adsorption on Au/BN resulted in a weak band at 510 nm while a relatively strong band at 558 nm was found under moisture. With moisture-CO co-feeding, the strong band at 558 nm remained and a new shoulder band in the region 322-360 nm (centered at 355 nm) appeared. No related band was observed on h-BN support under similar conditions (Figure S6). The shoulder band at 355 nm was obviously caused

by the interaction between CO and moisture on Au/BN. This is attributed to the absorbance of $^{*}CO(H_2O)_n$ species as discussed previously. The similar SPR band position under CO-H_2O and under H_2O suggests that H_2O dominates the charge transfer with metallic gold, corroborated with the relatively weak band intensity at 510 nm under dry CO.

Figure 7b shows how the bands observed under CO- H_2O would change when purging dry N_2 or dry O_2 at RT. After switching to dry N_2, both the shoulder band at 355 nm and the SPR band at 558 nm had negligible change. However, these two bands decreased significantly after switching to dry O_2 wherein the shoulder band vanished eventually. This indicates that the species contributing to the absorbance bands at 355 nm reacted with O_2.

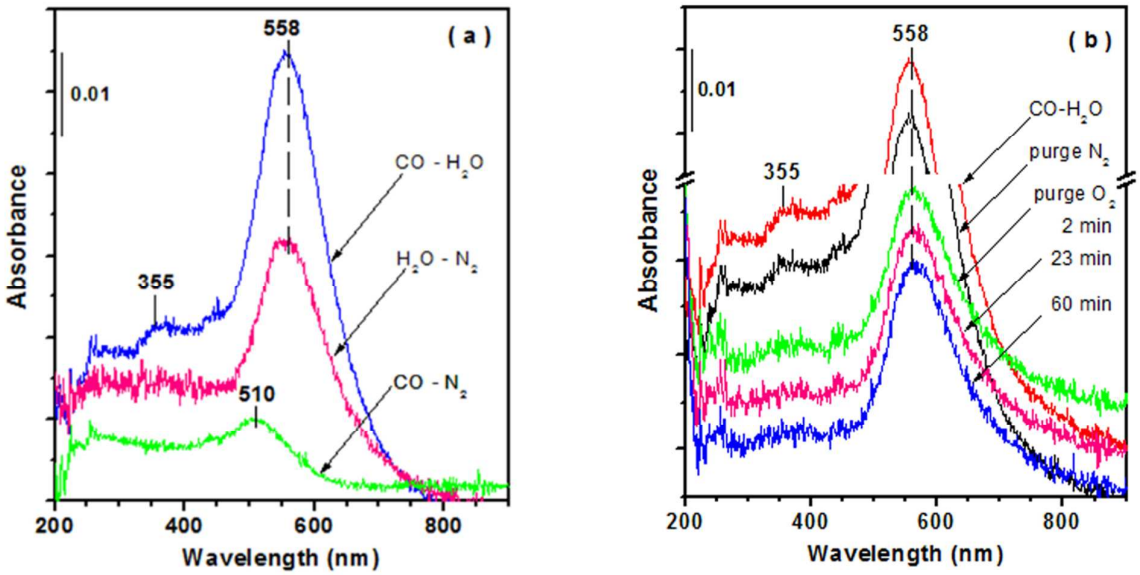

Figure 7. (a) In situ UV-Vis-DRS spectra of Au/BN under 1% CO, H_2O (100% RH), and 1% CO with moisture (100% RH) at RT; (b) Changes in the UV-Vis-DRS spectra of Au/BN at RT after switching the feed from CO-H_2O to dry N_2 flow or to dry O_2 flow. The reference spectrum is that of freshly pretreated Au/BN under dry N_2.

In situ UV-Vis-DRS spectra of Au/BN under moisture and O_2 flow are shown in Figure 8a. A weak band at 600 nm was found under nominal dry O_2, in contrast to the band at 558 nm under moisture only. With

O_2-H_2O co-feeding, the SPR band shifted to 567 nm and a new band at 374 nm appeared. An interaction between O_2 and H_2O is indicated by the new band and the shift of SPR band to new position in between that under O_2 and that under H_2O. Earlier reports proposed that a broad band at 360-370 nm occurs through charge transfer between hydroperoxyl ligand (-OOH) and Ti^{4+}, Fe^{3+}.[28,56,60-62] Therefore, we attribute the observed band at 374 nm to the formation of *OOH species on Au/BN and consequently, the SPR band at 567 nm indicates its interaction with Au.

Figure 8b shows how the bands related to *OOH changed when purging dry N_2 or dry CO. Both the charge transfer band and the SPR band retained their band position under dry N_2 purge; the SPR band decreased slightly in band intensity. However, both bands decreased in intensity and shifted to lower wavelength after switching to dry CO flow. This indicates the reactivity of *OOH with CO.

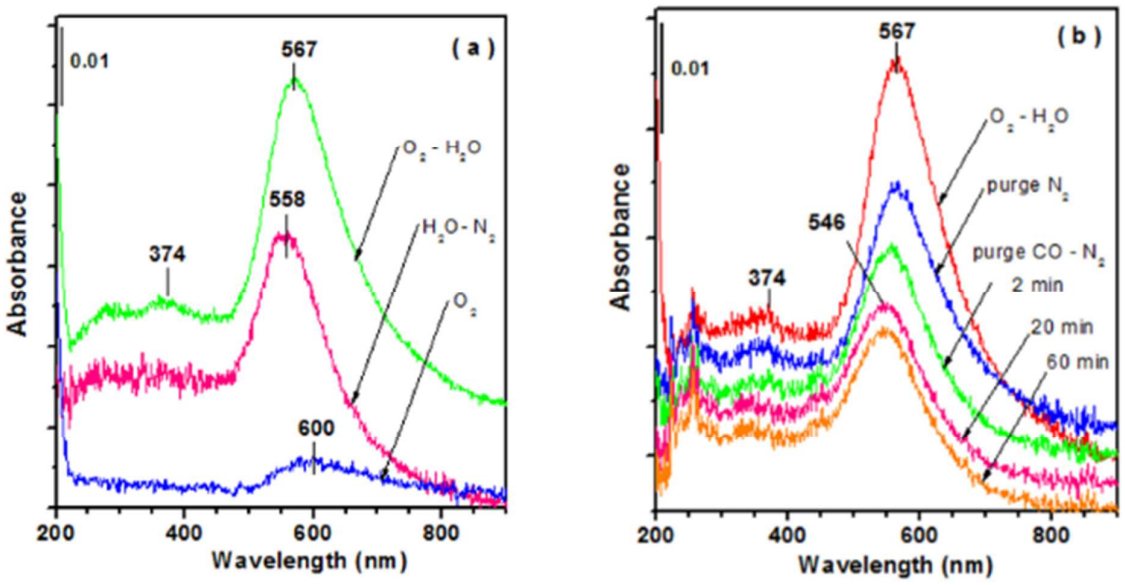

Figure 8. (a) In situ UV-Vis-DRS spectra of Au/BN under 20% O_2, H_2O (100% RH), and 20% O_2 with moisture (100% RH) at RT; (b) Changes in the UV-Vis-DRS spectra of Au/BN at RT after switching the feed from O_2-H_2O to dry N_2 flow and to dry CO flow. The reference spectrum is that of freshly pretreated Au/BN under dry N_2.

Figure 9 shows the comparison of in situ UV-Vis-DRS spectra during CO oxidation over Au/BN at RT under nominal dry and wet conditions. Under nominal dry CO oxidation conditions, the SPR band is located in between that under dry CO and that under dry O_2. No new band was found in the range of 250-450 nm. Under wet CO oxidation conditions, the SPR band is similar to that under H_2O-O_2, suggesting that the *OOH species dominate the charge transfer of Au. The band in the range from 250-450 nm presented under wet CO oxidation conditions seems to shift to somewhat higher wavelength compared to that under H_2O-O_2 and that under H_2O-CO.

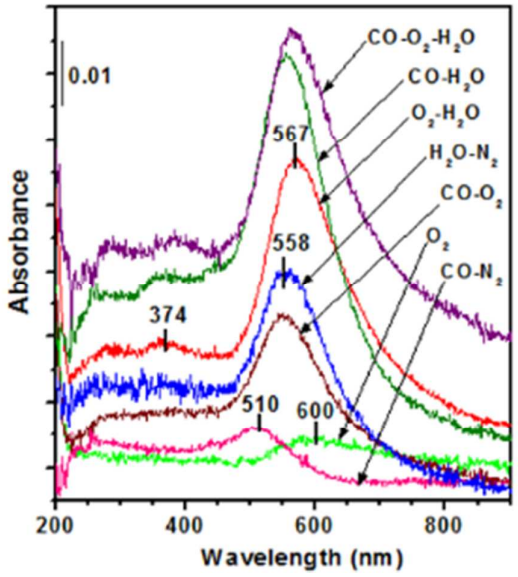

Figure 9. In situ UV-Vis-DRS spectra of CO oxidation over Au/BN at RT under nominal dry and wet (100% RH) conditions.

3. Discussion

The results in this and previous studies[5,7,8,22] demonstrate that H_2O acts as a co-catalyst to enhance CO oxidation over Au catalysts. The dependency of CO oxidation activity on H_2O content is continuous increase over Au/BN, not the typically observed volcano-shape dependency over oxide-supported Au catalysts.[5,7,8,22] This implies that how H_2O can influence CO oxidation over Au catalysts can be adjusted

by varying surface hydrophilicity, since BN surface is known more hydrophobic than the frequently used oxide supports.

Grant et al.[63] proposed that oxygen-terminated armchair sites are the active sites for oxidative dehydrogenation of propane at elevated temperature (480 ^{o}C), wherein vibrational bands at 1192 cm^{-1} (assigned to B-O) and ~3200 cm^{-1} (assigned to –OH on BN) were found significantly increased after the reaction. Although the 1192 cm^{-1} band assignment may be different [64-68], the proposed active sites may cause dehydrogenation of propane and oxygen can regenerate the active sites via oxidation of hydrated B-O and/or B-OH. This implies that edge sites of BN may interact with oxygen molecule and may lead to its activation. We did not find any significant band formation while flowing H_2O and H_2O+CO+O_2 over BN at RT in DRS-UV-Vis (Figure S6) and DRIFTS (Figure S7). Furthermore, no CO oxidation was detected when co-feeding H_2O with CO+O_2 over BN. This suggests that O_2 activation at the edge sites of BN may not be responsible for the observed activity over Au/BN at the conditions of this study.

Spectroscopic studies in this report show that H_2O causes changes in CO adsorption and O_2 adsorption which can consequently enhance CO oxidation over Au/BN. A new IR absorbance band at 2170 cm^{-1} is attributed to new surface intermediates from the interaction between CO_{ad} and H_2O, namely, $^{*}CO(H_2O)_n$. On the other hand, *OOH (hydroperoxyl) is observed when co-feeding moisture with O_2. This *OOH has been proposed from DFT calculation[20-23] as the key step to O_2 activation and to high CO oxidation activity. Both $^{*}CO(H_2O)_n$ and *OOH surface species are reactive toward CO_2 formation. The results of this study provide direct evidence for the role of H_2O in activating both CO_{ad} and O_{2ad}.

The observed 2170 cm^{-1} band in DRIFTS when co-feeding CO and moisture was previously attributed to *COOH. The formation of hydroxyl carbonyl intermediate is also studies in the electrochemical oxidation of CO over Au electrodes.[69,70] The presence of *COOH during gas phase CO oxidation over Au catalysts was first proposed by Bond and Thompson[9] involving Au^{3+}-OH. Kung and coworkers[10,11] also proposed *COOH as an intermediate that can lead to CO_2 formation and also carbonates causing catalyst deactivation; the proposed COOH was considered as formate and was formed via OH on cationic Au. Related assignments of IR absorbance band at around 2170 cm^{-1} to COOH are proposed to occur through interactions between CO and the abundant OH groups on oxides such as SiO_2, TiO_2, and CeO_2.[17,40,69]

However, there is no report of shift in ν_{OH} band when *COOH forms. More importantly, the interaction between OH and CO on Au surface is expected to cause a red shift in ν_{CO}[50] and therefore, the assignment of 2170 cm^{-1} band to ν_{CO} of *COOH is doubtful. Another attribution to the observed DRIFTS bands is $^{*}CO(H_2O)_n$ intermediate, of which no related report can be found on Au catalysts. However, recent reports mentioned that change in water clustering can be caused by surface functional group and the water cluster size can influence the H-bonding between water molecules and the possible proton transfer.[71,72] Thus, it seems reasonable to hypothesize that CO_{ad} can cause change in water cluster size which may subsequently change the chemistry of H_2O and CO_{ad}.

How O_2 can be activated over Au catalysts has been a long argued question. Recent theoretical studies[21-23] proposed that *OOH species is an active intermediate for CO oxidation over supported Au catalysts. The formation of *OOH through proton transfer from H_2O to O_{2ad} is found viable by DFT analysis. This *OOH species has also been studied in electrochemical oxygen reduction[73,74] as the key step for O_2 activation. However, direct experimental evidence in gas phase reaction system is scarce. The presence of $AuOOH{\cdot}xH_2O$ during gas phase CO oxidation was first proposed over Au-Fe catalyst based on Mossbauer spectroscopy.[19] IR bands of *OOH on TS-1 upon H_2O_2 exposure[26] and an absorbance band at 370 nm in UV visible spectra during propylene epoxidation over Au/TS-1[62] are reported. These are consistent with our spectroscopic observations. The proton transfer, $^{*}H_2O + {}^{*}O_2 \rightarrow {}^{*}OOH + {}^{*}OH$, leads to *OOH and *OH species. We shows that *OOH disappeared upon purging dry CO, suggesting a reaction between *OOH and CO_{ad}. However, the possibility that CO_{ad} interact with surface H_2O or OH may take place before reaction. Consequently, we cannot rule out the possibility that *OOH reacts with *COOH (or $^{*}CO(H_2O)_n$) forwarding CO_2. The reaction between *OOH and *COOH would regenerate *OH as proposed by Bond and Thompson.[9] Previous studies mentioned that *OH cannot be generated from H_2O adsorption on clean Au surface[43-45] but transient *OH can form on O-covered Au.[43,44] The transient *OH species from either the reaction between *OOH and *COOH (or $^{*}CO(H_2O)_n$) or the H_2O adsorption on O-covered Au may interact with CO_{ad} to form *COOH. Wu et al.[44] proposed that *OH groups on Au recombine to H_2O and O_{ad} upon heating. This can cause regeneration of H_2O, matching its role as a co-catalyst not reactant, and contribution to CO_2 formation since O_{ad} on Au surface is known reactive for CO

oxidation. We are working in combining with DFT calculations to elucidate a comprehensive reaction mechanism which will be reported in the near future.

When flowing CO, O_2, H_2O, CO-H_2O, or O_2-H_2O over Au/BN, changes in SPR absorbance band in the range 500 – 600 nm are obvious in UV-Vis-DRS spectra (with Au/BN under dry N_2 as the reference). This suggests that adsorbed species over Au surface cause changes in Au electron density. Under nominal dry conditions, co-feeding CO-O_2 resulted in a SPR band in between that of feeding only CO and of feeding only O_2 (Figure 9). However, the SPR band position under CO-O_2-H_2O feeds is nearly the same as that under O_2-H_2O. This suggests that the *OOH species dominates the charge transfer with Au, probably due to its adsorption strength and/or its abundance on Au surface. The intermediate *OOH is reactive leading to CO_2 formation, and the consequently formed *OH can also contribute to CO_2 formation through interaction with CO_{ad} to form *COOH[17,18] and/or recombination resulting in H_2O and O_{ad}.[44] It should be noted that if *OH is consumed only by interacting with CO_{ad} to form *COOH, there will be no way to regenerate H_2O through subsequent reaction between *COOH with O_{2ad}.

To the best of our knowledge, this study provides the first direct evidence that both $^*CO(H_2O)_n$ and *OOH species are formed on Au/BN and are active intermediates leading to CO_2 formation. Furthermore, the increasing CO oxidation over Au/BN with increasing moisture content up to 100% RH at RT can lead to design for moisture-tolerable Au catalysts. This may promote the applications of Au catalysts for CO abatement and CO detection under ambient conditions.

4. Conclusions

Au/BN prepared via a deposition method can catalyze CO oxidation at RT. The CO oxidation activity of Au/BN increases with increasing moisture content to 100% RH. In situ DRIFTS shows that an additional absorbance band at 2170 cm^{-1} appears when co-feeding moisture and CO in comparison to that under dry CO, indicating H_2O-enhanced CO adsorption. The formation of new intermediate, $^*CO(H_2O)_n$, is suggested, and the bands associated with the new species disappear upon purging O_2. Co-feeding O_2-H_2O results in the formation of hydroperoxyl (*OOH) intermediate as indicated by the observed absorbance bands of $\nu_{O\text{-}O}$ and $\delta_{OOH,}$ at 833 and 1220-1095 cm^{-1}, respectively, in DRIFTS. The hydroperoxyl species is

reactive when purging CO leading to CO_2 formation. In situ UV-Vis-DRS spectra give supporting evidences of the formation of these species and the reactivity. Moisture is not a reactant during CO oxidation over Au/BN at RT and its roles include the promotion and activation of molecularly adsorbed O_2 and of molecularly adsorbed CO, and the enhanced CO_2 formation activity from the observed surface intermediates of $^*OOH$ and $^*CO(H_2O)_n$.

AUTHOR INFORMATION

Corresponding Author: Shawn D. Lin

* Address: Department of Chemical Engineering, National Taiwan University of Science and Technology, Taipei 106, Taiwan, R.O.C.

Tel: +886-2-27376984

Fax: +886-2-27376644

E-mail: sdlin@mail.ntust.edu.tw

Author Contributions

The manuscript was written through contributions of all authors. All authors have given approval to the final version of the manuscript.

Supporting Information

The particle size distribution of gold on Au/BN, N_2 adsorption-desorption isotherm and moisture adsorption over h-BN and Au/BN. SEM images of h-BN and Au/BN. The dependency of steady state CO oxidation rate on moisture partial pressure, including supersaturation condition (P_{H2O} > 3.17 kPa). The comparison of H_2O adsorption on h-BN and Au/BN with some metal oxides based on BET model. In situ DRIFTS while introducing CO over Au/BN (solid lines) and h-BN (dotted lines) under wet (100% RH) conditions. In situ DRIFTS spectra of Au/BN when introducing moisture (100% RH) to nominal dry CO

oxidation reaction feed. In situ UV-Vis-DRS spectra of h-BN under 100% N_2, 20% O_2, H_2O (100% RH), 1% CO with moisture (100% RH) feedings, and CO oxidation in wet (100% RH) condition at RT. In situ DRIFTS of exposing h-BN with H_2O at RT vs. time, KBr as reference sample. In situ DRIFTS of CO, O_2 co-feeding with H_2O over h-BN (dot line - h-BN in N_2 as reference sample) and Au/BN (solid line - Au/BN in N_2 as reference sample) at RT in the range of 1450 – 1120 cm^{-1}

Acknowledgement

The authors gratefully acknowledge the financial support of Ministry of Science and Technology, Taiwan and partial support, under Top University Projects, from Ministry of Education, Taiwan.

References

(1) Lin, S. D.; Bollinger, M.; Vannice, M. A. *Catal. Lett.* **1993**, *17*, 245-262.

(2) Su, Y.-S.; Lee, M.-Y.; Lin, S. *Catal. Lett.* **1999**, *57*, 49-53.

(3) Haruta, M. *Cattech* **2002**, *6*, pp 102-115.

(4) Tsai, H.-Y.; Lin, Y.-D.; Fu, W.-T.; Lin, S. D. *Gold Bull.* **2007**, *40*, 184-191.

(5) Daté, M.; Haruta, M. *J. Catal.* **2001**, *201*, 221-224.

(6) Date, M.; Ichihashi, Y.; Yamashita, T.; Chiorino, A.; Boccuzzi, F.; Haruta, M. *Catal. Today* **2002**, *72*, 89-94.

(7) Okumura, M.; Tsubota, S.; Haruta, M. *Angew Chem. Int. Ed.* **2004**, *43*, 2129-2132.

(8) Ojeda, M.; Zhan, B.-Z.; Iglesia, E. *J. Catal.* **2012**, *285*, 92-102.

(9) Bond, G. C.; Thompson, D. T. *Gold Bull.* **2000**, *33*, 41-50.

(10) Costello, C.; Kung, M.; Oh, H.-S.; Wang, Y.; Kung, H. *Appl. Catal. A: Gen.* **2002**, *232*, 159-168.

(11) Costello, C.; Yang, J.; Law, H.; Wang, Y.; Lin, J.-N.; Marks, L.; Kung, M.; Kung, H. *Appl. Catal. A: Gen.* **2003**, *243*, 15-24.

(12) Henao, J. D.; Caputo, T.; Yang, J. H.; Kung, M. C.; Kung, H. H. *J. Phys. Chem. B* **2006**, *110*, 8689-8700.

(13) Boccuzzi, F.; Chiorino, A.; Tsubota, S.; Haruta, M. *J. Phys. Chem.* **1996**, *100*, 3625-3631.

(14) Manzoli, M.; Chiorino, A.; Boccuzzi, F. *Appl. Catal. B* **2004**, *52*, 259-266.

(15) Šmit, G.; Strukan, N.; Crajé, M. W. J.; Lázár, K. *J. Mol. Catal. A: Chem.* **2006**, *252*, 163-170.

(16) Wang, H. F.; Kavanagh, R.; Guo, Y. L.; Guo, Y.; Lu, G. Z.; Hu, P. *Angew. Chem. Int. Ed.* **2012**, *51*, 6657-6661.

(17) Chen, J.; Pidko, E. A.; Ordomsky, V. V.; Verhoeven, T.; Hensen, E. J. M.; Schouten, J. C.; Nijhuis, T. A. *Catal. Sci. Technol.* **2013**, *3*, 3042-3055.

(18) Zhang, S.; Li, X.-S.; Chen, B.; Zhu, X.; Shi, C.; Zhu, A.-M. *ACS Catal.* **2014**, *4*, 3481-3489.

(19) Finch, R. M.; Hodge, N. A.; Hutchings, G. J.; Meagher, A.; Pankhurst, Q. A.; Siddiqui, M. R. H.; Wagner, F. E.; Whyman, R. *Phys. Chem. Chem. Phys.* **1999**, *1*, 485-489.

(20) Bongiorno, A.; Landman, U. *Phys. Rev. Lett.* **2005**, *95*, 106102.

(21) Chang, C.-R.; Wang, Y.-G.; Li, J. *Nano Res.* **2011**, *4*, 131-142.

(22) Saavedra, J.; Doan, H. A.; Pursell, C. J.; Grabow, L. C.; Chandler, B. D. *Science* **2014**, *345*, 1599-1602.

(23) Chang, C.-R.; Huang, Z.-Q.; Li, J. *Nano Res.* **2015**, *8*, 3737-3748.

(24) McCandlish, E.; Miksztal, A. R.; Nappa, M.; Sprenger, A. Q.; Valentine, J. S.; Stong, J. D.; Spiro, T. G. *J. Am. Chem. Soc.* **1980**, *102*, 4268-4271.

(25) Kitajima, N.; Komatsuzaki, H.; Hikichi, S.; Osawa, M.; Moro-oka, Y. *J. Am. Chem. Soc.* **1994**, *116*, 11596-11597.

(26) Lin, W.; Frei, H. *J. Am. Chem. Soc.* **2002**, *124*, 9292-9298.

(27) Nakamura, R.; Imanishi, A.; Murakoshi, K.; Nakato, Y. *J. Am. Chem. Soc.* **2003**, *125*, 7443-7450.

(28) Huang, J.; Akita, T.; Faye, J.; Fujitani, T.; Takei, T.; Haruta, M. *Angew. Chem. Int. Ed.* **2009**, *48*, 7862-7866.

(29) Watanabe, K.; Taniguchi, T.; Kanda, H. *Nat. Mater.* **2004**, *3*, 404-409.

(30) Stehle, Y.; Meyer, H. M.; Unocic, R. R.; Kidder, M.; Polizos, G.; Datskos, P. G.; Jackson, R.; Smirnov, S. N.; Vlassiouk, I. V. *Chem. Mater.* **2015**, *27*, 8041-8047.

(31) Fielicke, A.; von Helden, G.; Meijer, G.; Pedersen, D. B.; Simard, B.; Rayner, D. M. *J. Am. Chem. Soc.* **2005**, *127*, 8416-8423.

(32) Leppelt, R.; Schumacher, B.; Plzak, V.; Kinne, M.; Behm, R. J. *J. Catal.* **2006**, *244*, 137-152.

(33) Liu, X.; Liu, M.-H.; Luo, Y.-C.; Mou, C.-Y.; Lin, S. D.; Cheng, H.; Chen, J.-M.; Lee, J.-F.; Lin, T.-S. *J. Am. Chem. Soc.* **2012**, *134*, 10251-10258.

(34) Venkov, T.; Fajerwerg, K.; Delannoy, L.; Klimev, H.; Hadjiivanov, K.; Louis, C. *Appl. Catal. A: Gen.* **2006**, *301*, 106-114.

(35) Manzoli, M.; Boccuzzi, F.; Chiorino, A.; Vindigni, F.; Deng, W.; Flytzani-Stephanopoulos, M. *J. Catal.* **2007**, *245*, 308-315.

(36) Hugon, A.; Kolli, N. E.; Louis, C. *J. Catal.* **2010**, *274*, 239-250.

(37) Hadjiivanov, K. I.; Klissurski, D. G. *Chem. Soc. Rev.* **1996**, *25*, 61-69.

(38) Hadjiivanov, K. *Appl.Surf. Sci.* **1998**, *135*, 331-338.

(39) Guzman, J.; Carrettin, S.; Corma, A. *J. Am. Chem. Soc.* **2005**, *127*, 3286-3287.

(40) Gaur, S.; Wu, H.; Stanley, G. G.; More, K.; Kumar, C. S. S. R.; Spivey, J. J. *Catal. Today* **2013**, *208*, 72-81.

(41) Venkov, T.; Klimev, H.; Centeno, M. A.; Odriozola, J. A.; Hadjiivanov, K. *Catal. Commun.* **2006**, *7*, 308-313.

(42) Romero-Sarria, F.; Penkova, A.; Martinez T, L. M.; Centeno, M. A.; Hadjiivanov, K.; Odriozola, J. A. *Appl.Catal. B* **2008**, *84*, 119-124.

(43) Quiller, R.; Baker, T.; Deng, X.; Colling, M.; Min, B.; Friend, C. *J. Chem. Phys.* **2008**, *129*, 064702-064709.

(44) Wu, Z.; Jiang, Z.; Jin, Y.; Xiong, F.; Huang, W. *J. Phys. Chem. C* **2014**, *118*, 26258-26263.

(45) Van Spronsen, M. A.; Weststrate, K.-J.; den Dunnen, A.; van Reijzen, M. E.; Hahn, C.; Juurlink, L. B. *J. Phys. Chem. C* **2016**, *120*, 8693-8703.

(46) Ferguson, J.; Weimer, A.; George, S. *Chem. Mater.* **2000**, *12*, 3472-3480.

(47) Sato, K.; Horibe, H.; Shirai, T.; Hotta, Y.; Nakano, H.; Nagai, H.; Mitsuishi, K.; Watari, K. *J. Mater. Chem.* **2010**, *20*, 2749-2752.

(48) Engeldinger, J.; Richter, M.; Bentrup, U. *Phys. Chem. Chem. Phys.* **2012**, *14*, 2183-2191.

(49) Leba, A.; Davran-Candan, T.; Önsan, Z. I.; Yıldırım, R. *Catal. Commun.* **2012**, *29*, 6-10.

(50) Shi En, F. *National Taiwan University of Science and Technology (in progress)* **2017**.

(51) Wang, Y.; Jiang, J.; Cheng, C.; Lin, S.; Lee, Y.; Chang, H. *J. Chem. Phys.* **1997**, *107*, 9695-9698.

(52) Jiang, J.-C.; Chang, J.-C.; Wang, B.-C.; Lin, S.; Lee, Y.; Chang, H.-C. *Chem. Phys. Lett.* **1998**, *289*, 373-382.

(53) Citra, A.; Chertihin, G. V.; Andrews, L.; Neurock, M. *J. Phys. Chem. A* **1997**, *101*, 3109-3118.

(54) Itoh, S. *Current Opin. Chem. Biol.* **2006**, *10*, 115-122.

(55) Valentine, J. S. *Chem. Rev.* **1973**, *73*, 235-245.

(56) Shearer, J.; Scarrow, R. C.; Kovacs, J. A. *J. Am. Chem. Soc.* **2002**, *124*, 11709-11717.

(57) Goebel, J. R.; Ault, B. S.; Del Bene, J. E. *J. Phys. Chem. A* **2001**, *105*, 11365-11370.

(58) Rogers, J. D.; Hillman, J. J. *J. Chem. Phys.* **1981**, *75*, 1085-1090.

(59) Li, M.; Wu, Z.; Overbury, S. H. *J. Catal.* **2011**, *278*, 133-142.

(60) Egan, J. W.; Haggerty, B. S.; Rheingold, A. L.; Sendlinger, S. C.; Theopold, K. H. *J. Am. Chem. Soc.* **1990**, *112*, 2445-2446.

(61) Gallard, H.; De Laat, J.; Legube, B. *Water Research* **1999**, *33*, 2929-2936.

(62) Chowdhury, B.; Bravo-Suárez, J. J.; Mimura, N.; Lu; Bando, K. K.; Tsubota, S.; Haruta, M. *J. Phys. Chem. B* **2006**, *110*, 22995-22999.

(63) Grant, J.; Carrero, C.; Goeltl, F.; Venegas, J.; Mueller, P.; Burt, S.; Specht, S.; McDermott, W.; Chieregato, A.; Hermans, I. *Science* **2016**, *354*, 1570-1573.

(64) Su, C.; Suarez, D. L. *Environ. Sci. Technol.* **1995,** *29,* 302-311.

(65) Sainsbury, T.; O'Neill, A.; Passarelli, M. K.; Seraffon, M.; Gohil, D.; Gnaniah, S.; Spencer, S. J.; Rae, A.; Coleman, J. N. *Chem. Mater.* **2014**, *26*, 7039-7050.

(66) Liao, Y.; Tu, K.; Han, X.; Hu, L.; Connell, J. W.; Chen, Z.; Lin, Y. *Sci. Rep.* **2015**, *5*, 14510.

(67) Peak, D.; Luther, G. W.; Sparks, D. L. Geochim. Cosmochim. Acta **2003**, *67*, 2551-2560.

(68) Tang, C.; Bando, Y.; Huang, Y.; Zhi, C.; Golberg, D. Adv. Funct. Mater. **2008**, *18*, 3653-3661.

(69) Edens, G. J.; Hamelin, A.; Weaver, M. J. *J. Phys. Chem.* **1996**, *100*, 2322-2329.

(70) Koverga, A. A.; Frank, S.; Koper, M. T. *Electrochim. Acta* **2013**, *101*, 244-253.

(71) Carrasco, J.; Hodgson, A.; Michaelides, A. *Nat. Mater.* **2012**, *11*, 667-674.

(72) Merte, L. R.; Bechstein, R.; Peng, G.; Rieboldt, F.; Farberow, C. A.; Zeuthen, H.; Knudsen, J.; Lægsgaard, E.; Wendt, S.; Mavrikakis, M. *Nat. Commun.* **2014**, *5*.

(73) Wang, Y.; Balbuena, P. B. *J. Phys. Chem. B* **2005**, *109*, 18902-18906.

(74) Anderson, A. B.; Albu, T. V. *J. Electrochem. Soc.* **2000**, *147*, 4229-4238.

Table of Contents Graphic